J Exp Biol Advance Online Articles. First posted online on 6 December 2016 as doi:10.1242/jeb.146605
Access the most recent version at http://jeb.biologists.org/lookup/doi/10.1242/jeb.146605

Stellate and Pyramidal Neurons in Goldfish Telencephalon Respond Differently to Anoxia and GABA Receptor Inhibition.

[1]Hossein-Javaheri, Nariman; [2]Wilkie, Michael P.; [3]Lado, Wudu E; [1]Buck, Leslie T.

[1]Department of Cell and Systems Biology, University of Toronto,

25 Harbord St, Toronto, ON, M5S 3G5.

[2]Department of Biology, Wilfred Laurier University,

75 University Avenue West, Waterloo, ON, N2L 3C5.

[3]Department of Neurobiology, University of Alabama at Birmingham,

1825 University Blvd, Birmingham, AL, 35294-2182

Corresponding author: les.buck@utoronto.ca

Key Words: Goldfish, anoxia, GABA, GABA receptors, E_{GABA}

Journal of Experimental Biology • Advance article

Summary Statement:

In this study we recorded electrophysiological characteristics of goldfish neurons and the role of GABA in the anoxic response for the first time.

Abstract:

With oxygen deprivation, the mammalian brain undergoes hyper-activity and neuronal death while this does not occur in the anoxia tolerant goldfish (*Carassius auratus*). Anoxic survival of the goldfish may rely on neuromodulatory mechanisms to suppress neuronal hyper-excitability. Since γ-aminobutyric acid (GABA) is the major inhibitory neurotransmitter in brain, we decided to investigate its potential role in suppressing the electrical activity of goldfish telencephalic neurons. Utilizing whole-cell patch-clamp recording we recorded the electrical activities of both excitatory (pyramidal) and inhibitory (stellate) neurons. With anoxia, membrane potential (V_m) depolarized in both cell types from -72.2mV to -57.7mV and from -64.5mV to -46.8mV in pyramidal and stellate neurons, respectively. While pyramidal cells remained mostly quiescent, action potential frequency (AP_f) of the stellate neurons increased 68 fold. Furthermore, the $GABA_A$ receptor reversal potential (E_{GABA}) was determined using the gramicidin perforated-patch clamp method and found to be depolarizing in pyramidal (-53.8mV) and stellate neurons (-42.1mV). Although GABA was depolarizing, pyramidal neurons remained quiescent since E_{GABA} is below the action potential threshold (-36mV pyramidal and -38mV stellate neurons). Inhibition of $GABA_A$ receptors with gabazine reversed the anoxia mediated response. While $GABA_B$ receptor inhibition alone did not affect the anoxic response, co-antagonism of $GABA_A$ and $GABA_B$ receptors (gabazine and CGP-55848) lead to generation of seizure-like activities in both neuron types. We conclude that with anoxia V_m depolarizes towards E_{GABA} which increases AP_f in stellate neurons and decreases AP_f in pyramidal neurons, and that GABA plays an important role in the anoxia-tolerance of goldfish brain.

Journal of Experimental Biology • Advance article

Introduction

During periods of oxygen deprivation ATP synthesis in anoxia-intolerant brain (mammals) halts and compromises the ability of the Na^+/K^+ ATPase pump to maintain neuronal ion gradients, leading to membrane depolarization (Hansen, 1985). The release of excitatory neurotransmitters (glutamate, aspartate) follows, leading to activation of α-amino-3-hydroxy-5-methyl-4-isoxazolepropionic acid (AMPA) and N-Methyl-D-aspartate (NMDA) receptors (Sattler and Tymianski, 2000). Subsequent calcium (Ca^{2+}) influx through NMDA receptors causes further depolarization of membrane potential, and activates intracellular Ca^{2+} dependent signaling cascades, which leads to neuronal hyper-excitability and eventually, excitotoxic cell death (Sattler and Tymianski, 2000). As anoxia eliminates oxidative phosphorylation, the glycolytic pathway becomes the major source of ATP produced by the brain, generating less than $1/10^{th}$ of the ATP produced under normoxic conditions (Hochachka, 1986). The ATP shortfall is particularly problematic for neurons, since action potential propagation, consequent activation of output synapses and maintenance of neuronal ion gradients are metabolically expensive events, consuming approximately 60% of the total brain ATP turnover (Erecinska and Silver, 1994). Anoxia-tolerant organisms, such as the western painted turtle (*Chrysemys picta*), avoid anoxia-mediated cellular injury by reducing not only ATP synthesis by over 90% (Bickler and Buck, 2007) but also reducing ATP demand, indeed in the case of turtle cortical pyramidal neurons, an anoxia-mediated 60 – 70% reduction in action potential frequency has been reported (Pamenter et al. 2011).

There are three hypotheses that encompass the events that lead to a large decrease in metabolic rate such as that exhibited by anoxic-tolerant species; these are the Metabolic Arrest (MA), Channel Arrest (CA) and Spike Arrest (SA) Hypotheses (Hochachka 1986, Lutz et al. 1992). The MA hypothesis generally describes events leading to a reduction in ATP supply while the CA hypothesis is specific to a reduction in ion channel conductance leading to a reduction in ATP demand. The SA hypothesis is specific to neurons or excitable tissues and entails a reduction in action potential frequency that lead to a reduction in ATP demand and therefore a reduction in ATP supply (Hochachka et al. 1996). Neurons function within an integrated network; therefore, mechanisms regulating metabolic rate are also likely to occur at the network level. Specifically, with the onset of anoxia some neurons may be

Journal of Experimental Biology • Advance article

activated in order to inhibit other neurons. We found evidence of this in anoxia-tolerant turtle cortical neurons where glutamatergic pyramidal neurons undergo spike arrest as a result of an increase in inhibitory $GABA_A$ receptor currents (Pamenter et al. 2011). However, we have not recorded directly from the likely source of the increased GABA levels – stellate interneurons.

Stellate neurons are smaller than pyramidal neurons and are more difficult to patch clamp in the turtle cortex (Connors and Kriegtein, 1986); therefore, our present goal is to develop a brain slice model in which stellate neurons could be reliably patched to obtain recordings during a normoxic to anoxic transition. Since the reversal potential (E_{GABA}) for the $GABA_A$ receptor is depolarized relative to membrane potential in the turtle pyramidal neurons we also set out to determine E_{GABA} in both goldfish stellate and pyramidal neurons. We hypothesize that with the onset of anoxia stellate neuron membrane potential will depolarize towards E_{GABA} and action potential frequency (AP_{freq}) will increase. Furthermore, we hypothesize that membrane potential will depolarize towards E_{GABA} and whole cell conductance will increase in pyramidal neurons but AP_{freq} will decrease.

Methods

Animal. This study was approved by the University of Toronto Animal Care Committee and conforms to the relevant guidelines issued by the Canadian Council of Animal Care regarding the care and use of experimental animals. Common goldfish (*Carassius auratus*), weighting 50-100gm were purchased from a commercial supplier (AQUAlity Tropical Fish Wholesale, Mississauga, ON) and held in flowing dechlorinated City of Toronto tap water at 18°C at the University of Toronto.

Golgi Staining. Whole goldfish brain was removed from the cranium following decapitation and the entire brain underwent Golgi staining. This technique reveals fine structures of neurons, glia and their processes, allowing a better understanding of cellular morphology along with their orientation and location in cortical slices (Melendez *et al*., 2009). Tissue was fixed in 10% formalin for 2 days followed by fixation in 3% $K_2Cr_2O_7$ for 1 day and 2% $AgNO_3$ for another 2 days (Olgue *et al*., 2015). The telencephalon was separated from the rest of the brain and sliced into 100µm thick axial slices using a Leica VT1200S vibratome. Slices

were collected using a soft brush, placed on a microscope slides, cover-slipped and stored at 4°C

Whole-Cell Electrophysiology. Telencephalon dissection, tissue preparation and whole-cell patch patch-clamp recording methods are described elsewhere (Wilkie *et al*., 2008). In short, the whole brain of the goldfish was removed from the cranium after decapitation and was placed in oxygenated ice-cold 4°C artificial cerebrospinal fluid (aCSF) containing (in mM): 20 $NaHCO_3$, 118 NaCl, 1.2 $MgCl_2.6H_2O$, 1.2 KH_2PO_4, 1.9 KCl, 10 HEPES-Na, 10 D-Glucose and 2.4 $CaCl_2$ (pH 7.6, adjusted with HCl); osmolarity 285-290 mOsm). Both lobes of telencephalon were then dissected from the rest of the brain while in the chilled aCSF. Each telencephalon lobe was glued to a sectioning plate on a vibratome's slicing chamber using cyanoacrylate glue ("Krazy Glue") and was filled with 4°C aCSF. Isolated goldfish telencephalon was cut to 300µm slices using a VT1200S vibratome (Leica, Richmond Hill, ON). Slices were lifted out of the chamber and were stored in vials of oxygenated aCSF for no longer than 48 hours. Slices remained physiologically viable up to 48 hours of preparation (Wilkie, 2008). During each experiment, individual telencephalon slices were perfused with either oxygenated (99% O_2, 1% CO_2) or anoxic (99% N_2, 1 %CO_2) aCSF (composition described above), and whole-cell recordings were performed using the voltage clamp method with 9-11MΩ borosilicate glass pipette electrodes (Harvard Apparatus LTD, Holliston, MA) containing the following (in mM): 120 K-gluconate, 10 KCl, 15 sucrose, 2 Na_2ATP, 0.44 $CaCl_2$, 1 EGTA and 10 HEPES-Na (pH, 7.6 adjusted with KOH; Osmolarity 285-290mOsm). The electrode was connected to a CV-4 headstage (Gain: 1/100U, Axon Instruments, Sunnyvale, CA) and an AXOPATCH 1D patch-clamp amplifier (Axon Instruments, Sunnyvale, CA). A whole-cell patch configuration was established by voltage-clamping the recording potential to -60mV and applying negative pressure after a 1-20 GΩ seal was established. All seals were obtained using the blind-patch technique (Blanton *et al*., 1989). Whole-cell capacitance was compensated, typical whole-cell access resistance (R_a) was 30-40MΩ and series resistance (R_s) was not greater than 50MΩ. R_a was monitored periodically and data were discarded if it changed by 10-15MΩ. Electrophysiological recordings were performed on pyramidal neurons and stellate neurons in goldfish telencephalon. The cerebral cortex of fish, amphibians and reptiles is characterized by three layers in which the pyramidal neurons are excitatory glutamatergic cells and the stellate neurons are primarily

GABAergic and inhibitory, providing feed-forward and feedback inhibition to pyramidal cells (Shepherd, 2011; Larkum *et al*., 2008). Electrophysiologically, the two cell types were differentiated in goldfish telencephalon by their responses to somatic current injections which produce trains of action potentials. If accommodation occurred quickly, the cell was distinguished as a pyramidal neuron and if no accommodation was observed, the cell was differentiated as stellate neurons. Further, neural morphology was determined by filling the microelectrode solution with 5% Lucifer Yellow (LY) in 2M LiCl. LY was ejected by steady hyperpolarizing current for 5min after completion of the experiment (Connors and Kriegtein, 1986; Shin and Buck, 2003). Spontaneous electrical activity was recorded for approximately 1hr (5-10min normoxia, 30min anoxia, 20min recovery) from pyramidal and stellate neurons. Action potential threshold (AP_{th}) was determined by injecting current in a ramp manner in 1nA steps until an AP was elicited. G_w was measured by clamping neurons at voltage steps from -90 to -30mV in 10mV increments, lasting 200ms each. Current amplitudes were measured between 135-145ms and a slope conductance according to the current-voltage (I/V) relationship was determined (Pamenter *et al*., 2011).

Perforated-Patch Electrophysiology. We utilized the gramicidin perforated-patch technique to determine GABA reversal potential (E_{GABA}) without perturbing neural Cl^- gradients. Micropipette tips were front-filled with electrode recording solution by applying suction to the back of the pipette for 30 sec, then back-filled with a solution of 13µg/ml gramicidin in DMSO dissolved in electrode solution. G_w recordings and I/V relationships were analyzed by taking the linear regression of each line before and during 2mM GABA application. E_{GABA} was estimated by measuring the voltage at which the I/V relationships, before and during GABA application, intersected (Watanabe *et al*., 2009). Using the Nernst equation and the known extra-cellular [Cl^-] we estimated the intracellular [Cl^-] from E_{GABA}. Calculated E_{GABA} was achieved by deducting conductance values, pre and post GABA application, and plotting the results on an I/V curve.

Pharmacology. Goldfish telencephalon slices were perfused with pharmacological modifiers as specified in the *Results* through a fast step perfusion system (VC-6 perfusion valve controller and SF-77B fast-step perfusion system; Warner Instruments, Hamden, CT). Possible involvement of the GABAergic system in the anoxic response was investigated by application of $GABA_A$ and $GABA_B$ receptor antagonists, 25µM SR95531 gabazine (GZ), 5µM

CGP-55848 (CGP) and 100µM bicuculline (BIC) during anoxia. Changes in membrane potential (V_m) and action potential frequency (AP_f) of pre and post drug application were compared. AMPA and NMDA receptors were blocked using 25 µM of 6-cyano-7-nitroquinoxaline-2, 3-dione (CNQX) and 25 µM (2*R*)-amino-5-phosphonovaleric acid (APV), respectively. Voltage gated sodium channels were blocked with 1µM tetrodotoxin (TTX). The GABA reversal potential E_{GABA} was obtained by perfusing cortical slices with 2mM GABA. All chemicals were obtained from Sigma-Aldrich Canada Ltd (Oakville, ON) except CGP-55848 and TTX which were obtained from Tocris Cookson (Bristol, UK).

Statistics. Electrophysiological data were analyzed using a SigmaPlot software package version 11.0 (Systat Software, Inc., San Jose, CA, USA). All data were tested for normality and equal variance and an analysis of variance (repeated measure ANOVA) was used for between-group comparisons where appropriate. *Post hoc* analyses consisted of Holm-Sidak or Tukey's. Data are expressed as mean±S.E.M; n-values represent a recording from a single cell from a single telencephalic slice of a single goldfish. $P<0.05$ was considered statistically significant.

Results

Goldfish telencephalic neurons are divided into distinct medially and laterally localized regions.

Golgi stain and fluorescent imaging revealed that goldfish telencephalon neurons were located in two distinct regions. First neural populations located at the lateral regions were spread into distinct layers (Figure 1A). For simplicity, we divided them into three types. The first type had a triangular shaped soma with dendritic fields extending away from the cell body in both apical and basal directions (Figure 1B, 1D). Their dendritic extensions were large with medial projections towards the center of the slice. With application of a suprathreshold current pulse, these neurons showed rapid adaptation and fired distinct action potentials followed with hyperpolarization (Figure 1F). Cells with these characteristics were identified in painted turtle cortex as pyramidal neurons (Connorrs and Kriegstein, 1986).

The second cell type in this region had a small (~25µm) and circular soma with bi-lateral projections extending away from the cell body (Figure 1C). It appeared that these cells were more localized and had little branching on their dendritic tree (Figure $1E_{ii}$). Type three cells had a more oval shaped cell body which was larger than type two cells (~50µm) (Figure $1E_{i}$). Similar to pyramidal neurons, they sent their projections medially and had large dendritic fields. Physiologically, both type two and three cell types showed little or no spike frequency accommodation in response to suprathreshold current. Action potentials were generated continuously and had equal amplitude (Figure 1G). This physiological morphology has been associated with stellate neurons (Connors and Kriegstein, 1986). The second population were part of *area dorsalis telencephali pars centralis* (*Dc*) located at the center of the slice and was isolated from the lateral region (Peter and Gill, 1975). *Dc* contained both pyramidal and type three stellate neurons; however, no type two stellate neurons were observed. Perhaps due to their small size, type two stellate neurons were encountered only twice. Hence data collected from these cells was excluded from the data set. Both pyramidal and stellate cells had large dendritic trees and were highly interconnected. In this experiment, the term "stellate neurons" refer to the type three stellate cells.

Pyramidal and stellate neurons respond differently to anoxia.

Pyramidal neurons are the primary excitatory neurons in the turtle cortex and are the major consumers of ATP (Howarth *et al*., 2010). A reduction in excitability of these neurons is crucial to tolerance of anoxia and ischemia and energy conservation (Pamenter *et al*., 2011; Hogg *et al*., 2015). Inhibition is not independent from the rest of the cortex and if GABAergic stimulation is responsible for suppression of neuronal excitability, the inhibitory stellate cells should show greater excitation with anoxia. Under passive recording conditions (I=0) it was observed that pyramidal neurons were mostly quiescent and membrane potential (V_m) was maintained at -72.18±2.3mV during normoxia. V_m depolarized to -57.7±1.6mV after 30 minutes of anoxia (p=0.01, n=14) and repolarized to -64.22±2.6mV after 20 minutes of normoxic recovery (p=0.08, n=14). Despite V_m depolarization, these cells did not generate an action potential (Figure 2, A, E and F). However, a small population of pyramidal neurons were more depolarized and active during normoxia (V_m= -60.5±1.6mV, AP_f = 0.51±0.03Hz). In these cells anoxic treatment caused a depolarization of V_m to -53±1.08mV (p=0.04, n=4) and AP_f

decreased to 0.1±0.06Hz ($p<0.001$, n=4). With normoxic recovery, V_m hyperpolarized to -55±2.6mV; however, this was not significantly different form anoxic V_m; AP_f increased to 0.24±0.1Hz ($p=0.003$ from anoxia to recovery, n=4) (Figure 2, D, H and G). Similar to pyramidal neurons, V_m depolarized from -64.54±1.05mV to -46.86±1.2mV and repolarized to -53 ±2.65mV in stellate neurons during a normoxic to anoxic transition and recovery ($p=0.02$ for normoxia to anoxia and $p=0.03$ for anoxia to recovery, n=11). Unlike pyramidal neurons, stellate neurons generated action potentials with anoxia and action potential frequency (AP_f) increased from 0.03±0.009Hz to 2.04±0.12Hz ($p<0.001$, n=11). AP_f was reduced to 0.13±0.03Hz with normoxic recovery ($p<0.001$, n=11) (Figure 2, B, E and F). Application of AMPA and NMDA receptor antagonists (CNQX 25µM and APV 25µM, respectively) did not suppress action potentials; however, 1 µM TTX abolished them (data not shown). Furthermore, both pyramidal and stellate neurons showed an ~60% increase in whole cell conductance (G_w) with anoxia. These changes were from 1.75±0.34nS to 2.83±0.17nS in pyramidal neurons ($p=0.04$, n=7) and 1.27±0.15nS to 2.01±0.16nS in stellate cells ($p=0.07$, n=8) (Figure 2, G).

Membrane potential shifts towards E_{GABA} with anoxia.

Activation of $GABA_A$ receptors leads to a Cl^- flux in the direction of the reversal potential (E_{Cl^-})(Blaesse et al., 2009). Since $GABA_A$ receptors are predominantly permeable to Cl^-, the GABA reversal potential (E_{GABA}) and E_{Cl^-} should be similar (Errington et al., 2014). We measured E_{GABA} in goldfish telencephalic neurons to better understand the relationship between V_m and E_{GABA}. In order not to perturb neuronal Cl^- gradients we used the gramicidin perforated-patch technique to determine E_{GABA}. Addition of 2mM GABA during normoxia increased V_m in telencephalic neurons by 20±2.6mV (n=8 for pyramidal and n=8 for stellate neurons, $p<0.001$) which returned to baseline after approximately 10min post GABA application (Figure 3, A). In pyramidal neurons, stepwise current injection generated action potentials in the absence of GABA but not in the presence of GABA (Figure 3, B). Similarly, stellate neurons showed suppressed activity with GABA application; however, with increased current injection, these neurons were capable of generating action potentials (Figure 3, C). Furthermore, G_w was recorded before and after GABA application and a current-voltage (I/V) relationship was constructed. GABA increased G_w and the intersection point between the two I/V curves was taken as the E_{GABA} (Figure 3, D). E_{GABA} was more depolarized in

stellate neurons than pyramidal cells, -42.1±2.3mV and -53.80±2.63mV, respectively. By obtaining the E_{GABA} values and utilizing the Nernst equation, we were able to calculate intracellular [Cl^-]. The $[Cl^-]_i$ was ~15.1mM and ~24mM in pyramidal and stellate neurons, respectively. As demonstrated previously G_w increased with anoxia from 3.96±0.95nS to 6.84±0.61nS ($p<0.001$, n=5). Addition of GABA appeared to increase G_w during normoxia; however, this increase was not significant (G_w= 5.49±0.86nS, p=0.3, n=5). With anoxia, G_w increased to 8.49±0.2nS which was significantly different from anoxia without GABA (p=0.02, n=5) and from normoxia with GABA ($p<0.001$, n=5) (Figure 3, E).

Anoxic V_m depolarization is reversed by inhibition of $GABA_A$ and $GABA_B$ receptors.

In order to investigate the possible role of GABA in defence against anoxia-mediated damage in goldfish telencephalic neurons, we blocked $GABA_A$ and $GABA_B$ receptors under anoxic conditions. During anoxia pyramidal neuron V_m hyperpolarized with application of 25µM of the $GABA_A$ receptor inhibitor SR95531 (Gabazine/GZ) from -56.54±1.7mV to -64.77±1.9mV and depolarized back to -55.15±1.36mV with normoxic recovery ($p<0.001$, n=6) (Figure 4, A and D). In anoxic stellate neurons GZ also hyperpolarized V_m, from -46.8±2.1mV to -58.54±2.1mV ($p<0.001$, n=5) and AP_f decreased from 2.04±0.12Hz to 0.155±0.01Hz ($p<0.001$, n=5) (Figure 4, B and E, AP_f not shown). These changes were reversed with the termination of GZ application. Bicuculline also hyperpolarized V_m to -68.82±1.7mV and -56.8±1.97mV in pyramidal and stellate neurons, respectively (n=3, $p<0.001$, data not shown). No significant difference was observed between bicuculline and gabazine in reversal of the anoxic response. Even though the $GABA_B$ receptor antagonist CGP-55848 (CGP) alone did not change V_m or AP_f in either cell type (V_m= -53.97±2.24mV for pyramidal and V_m=-47.74±2.83mV, n=4), co-antagonism of $GABA_A$ and $GABA_B$ receptors, significantly influenced neuronal excitability (Figure 4, E). GZ+CGP initially hyperpolarized V_m similar to what was observed with GZ perfusion. However, shortly after membrane potential depolarized significantly (V_m=-36.58±1.62, $p<0.001$, n=4; and -34.25±5.9mV $p<0.001$, n=5 for pyramidal and stellate neurons, respectively) and generated sudden, seizure-like action potentials (Figure 4, C and D). Furthermore, AP_f increased in pyramidal neurons from quiescent to 2.23±0.09Hz (n=4, $p<0.001$). The increase in AP_f was not significantly different in stellate neurons (AP_f=2.13±0.02Hz, n=5) (Figure 4, E). Even though AP_f drastically increased with GZ+CGP application, in some neurons (n=5) membrane potential

hyperpolarized to the pre-anoxia level, neurons became quiescent and stepwise current injection failed to generate an action potential (data not shown). The rest (n=4) however, did not recover after CGP+GZ application and continued to generate seizure-like action potentials until loss of membrane potential that is associated with neuronal death (Figure 4, C).

$GABA_{A/B}$ receptor antagonism significantly affected whole-cell conductance (G_w) in both pyramidal and stellate neurons. Anoxia increased G_w from 3.96±0.95nS to 6.84±0.62nS ($P<0.001$). Blocking the $GABA_A$ receptor with GZ had no significant effect on normoxic G_w (2.83±0.33nS, $p=0.071$) but it did significantly block the anoxia-mediated increase (3.87±0.39nS, $p<0.001$). Normoxic application of CGP alone did not have an effect on G_w (4.1±0.56nS, $p=0.81$) and application of CGP alone during the anoxic period did not suppress the anoxia-mediated increase (5.43±0.59nS, $p=0.27$). Co-application of GZ+CGP did not affect normoxic G_w (3.48±0.18nS, $p=0.43$) but did significantly bock the anoxia mediated increase in G_w (3.7±0.26nS, $p<0.001$). This suggests that the increase in conductance during anoxia is dependent on the activation of $GABA_A$ receptors and that GABA is likely responsible for anoxic depolarization (Figure 4, F). G_w measurments were conducted on anoxic and normoxic controls and ones treated with GZ, CGP and GZ+CGP, each with 5 replicates. Since the change in G_w was similar for both neuronal types the pharmacological responses were combined. Data are presented as the combined responses of pyramidal and stellate neurons.

Discussion

In this study we investigate the role of GABAergic neurotransmission in the telencephalon of the naturally anoxia-tolerant goldfish, *Carassius auratus*. We show that anoxia depolarizes the membrane potential of both stellate and pyramidal neurons towards the $GABA_A$ receptor reversal potential (E_{GABA}) which is reversed by application of a $GABA_A$ receptor ($GABA_AR$) blocker. Interestingly, depolarization by increasing $GABA_A$ receptor currents decreases pyramidal cell AP frequency (AP_f) while it increases the AP_f of stellate neurons. Furthermore, we show $GABA_B$ receptors ($GABA_BR$) are also important in anoxic survival since inhibition of both $GABA_{A/B}$ receptors induce seizure-like activities in telencephalic neurons and apparent cell death. GABA is the primary inhibitory

neurotransmitter in the mature mammalian central nervous system (CNS) and an increase in the extracellular [GABA] seems to be a common response to anoxia in anoxia-tolerant organisms (Krnjevic, 1997; Nilsson and Lutz 2004; Bickler and Buck, 2007). In the anoxia tolerant turtle brain (*Chrysemys picta bellii, Trachemys scripta elegans*) [GABA] increases by 80 fold, suppressing whole brain electrical activity by 75-95% (Lutz and Nilsson, 1997). This is strongly mediated by both $GABA_A$ and $GABA_B$Rs which are critical to anoxic survival of turtle cortical neurons (Pamenter *et al*., 2011). While turtles become quiescent and enter a stage of minimal activity, goldfish and crucian carp remain slightly active in anoxic waters (Bickler and Buck, 2007). Compared to levels in turtle brain, the anoxia-mediated increase in extracellular [GABA] in crucian carp brain is quite modest and doubles after 5 hours of anoxia (Hylland and Nilsson, 1999). Furthermore, with anoxia GABA removal from the extracellular space is significantly reduced since the expression of GABA transporter proteins (GATs) decreases by 80%, increasing the effective extracellular [GABA] further (Ellefsen *et al*., 2009). We observed a significant increase in neuronal membrane potential (V_m) with anoxia. This depolarization leads to action potential (AP) propagation in stellate neurons while pyramidal neurons remain silent. An increase in AP frequency of stellate neurons seems controversial to energy conservation within a low environmental oxygen; however, inhibitory neurons consume significantly less energy than excitatory neurons and there are about 10 fold fewer (Howarth *et al*., 2010). In a study by Hylland and Nilsson (1999), running a high [K^+] ringer solution through a microdialysis probe to depolarize the surrounding tissue caused the extracellular [GABA] to increase 14 times, while extracellular [glutamate] doubled. This suggests that the potential for GABA release in crucian carp telencephalon is significantly greater than that for glutamate, resulting in greater GABA release in response to equal amounts of stimulation. If we consider the similarities between the telencephalon of teleost fish and mice hippocampus, the number of excitatory synapses are approximately 18 fold greater than inhibitory ones (Megias *et al*., 2001; Muller, 2012). Therefore, as a defence mechanism in goldfish telencephalic neurons, a small population of neurons with high release potential and lower energy requirements are activated to suppress the larger population of excitatory neurons and conserve energy.

In our experiment, blocking NMDA and AMPA receptors failed to suppress AP firing in stellate neurons while tetrodotoxin blocked AP's completely. Therefore, we hypothesized

that pathways other than excitatory glutamatergic signaling, such as GABAergic pathways, are responsible for V_m depolarization during anoxia. Indeed, blocking $GABA_A$Rs with GZ reversed anoxic depolarization of V_m and prevented the anoxia-mediated increase in whole-cell conductance (G_w). Under physiological conditions, $GABA_A$Rs are highly permeable to both Cl^- and HCO_3^-; however, the channels are considerably more permeable to Cl^- than HCO_3^- (Cl^-/ HCO_3^- permeability: 5/1) and thus, the majority of charge transfer following channel activation is Cl^- mediated (Errington et al., 2014). Therefore, we conclude that the anoxic increase in G_w is largely due to the movement of anions.

Measurements of the GABA reversal potential (E_{GABA}) revealed that V_m shifts towards a depolarizing E_{GABA} with anoxia and induces action potentials in stellate neurons but not in pyramidal cells. This is consistent with a previous report showing exogenous GABA can depolarize goldfish telencephalic GnRH neurons (Nakane and Oka, 2010). By moving V_m to the $GABA_A$ receptor reversal potential in pyramidal neurons the potential difference between the intracellular and extracellular environments is decreased, which significantly reduces energy in the form of ATP required to maintain ionic gradients (Edwards *et* al., 1989). Although GABA is depolarizing, it remains inhibitory since it activates an inhibitory shunt that maintains V_m below the threshold potential (Pamenter *et al*., 2011). E_{GABA} is primarily determined by the Cl^- gradient where K^+-Cl^- contransporter 2 (KCC2) and Na^+-K^+- Cl^- cotransporter 1(NKCC1) set the reversal potential and driving force of anions currents mediated by $GABA_A$Rs (Blaesse et al., 2009). For GABA to have a depolarizing effect, the intracellular [Cl^-] must be relatively high (20-25mM) so that an efflux of Cl^- occurs via $GABA_A$Rs (Ben-Ari *et al*., 2002). We found that intracellular [Cl^-] is relatively high in goldfish telencephalic neurons and approximately 1.5 times greater in stellate neurons than in pyramidal neurons. As a result, activation of $GABA_A$Rs, leads to a greater efflux of Cl^- and further depolarization in stellate neurons compared to pyramidal neurons. Cl^- flow occurs through both synaptic (phasic) and extrasynaptic (tonic) GABARs (Blaesse et al., 2009). Localization of $GABA_A$Rs has not been investigated in goldfish neurons; however, crucian carp neurons express the gamma subunit which is necessary for phasic currents and delta subunits which in mammalian brain is extrasynaptic (Mody, 2001; Ellefsen *et al*., 2009). By applying gabazine, we likely inhibited the activity of phasic currents since gabazine has a greater affinity for synaptic $GABA_A$Rs (Mody, 2001). Application of bicuculline

hyperpolarized membrane potential of both pyramidal and stellate neurons and reduced action potential frequency in stellate neurons similar to gabazine. However, bicuculline blocks both phasic and tonic $GABA_A$Rs (Ueno *et al*., 1997); suggesting that the anoxic response is primarily mediated through the activity of the synaptic receptors. Anoxia-tolerant turtle brain differs from goldfish since anoxia induces large phasic GABA currents and a 50% increase in tonic current (Hogg *et al*., 2015). Large phasic GABAergic currents were only observed in a single goldfish pyramidal neuron recordings (1/47 attempts). Perhaps formation of such currents requires an intact circuitry or is localized to a specific cortical region. Since our electrophysiological recordings were from brain slices, the circuitry might have been disrupted (Dukoff *et al,* 2014, Hogg *et al*., 2015). Furthermore, all the recordings utilized the blind-patch technique which prevents clear localization of the areas populated with neurons that induce large GABA mediated currents (Blanton *et al*., 1989). Due to such limitations and inability to frequently record GABA induced currents, it is not possible to state to what degree tonic $GABA_A$Rs are involved in the anoxic response in the goldfish brain.

Blocking $GABA_B$Rs alone did not affect V_m or AP_f and changes in G_w were not as strong as that during $GABA_A$R inhibition. These receptors are slow acting (100-500ms) G-protein coupled inwardly-rectifying potassium channels (GIRKs) and mediate prolonged neural inhibition by increasing K^+ efflux via K^+ channels (GIRKs) post-synaptically and inhibiting voltage-gated Ca^{2+} channels pre-synaptically (Gassmann and Bettler, 2012). $GABA_B$R activity is strongly mediated by intracellular messenger mechanisms (Kuramoto *et al*, 2007). With anoxia or shortage of ATP, certain intracellular signaling proteins, such as AMP-dependent protein kinase (AMPK) are activated due to an increase in [AMP] (Carling, 2005). AMP has a critical role in maintaining cellular and systemic energy balance and promoting glycolysis (Stenslokken, 2008). Through phosphorylation AMPK strongly enhances $GABA_B$R activity, allowing a greater K^+ efflux via GIRKs (Kuramoto *et al*, 2007). Anoxic exposure significantly increases AMPK phosphorylation in crucian carp brain (Stenslokken, 2008).

In this experiment we were able to show that inhibition of both $GABA_{A/B}$ receptors leads to sudden, uncontrollable electrical activity and a paroxysmal depolarizing shift (PDS). PDS is a manifestation of neural epilepsy that is in contrast to endogenous burst firing as it is

network driven (Johnston and Brown, 1984). In some neurons V_m did not return to base line and seizure-like activities persisted. In others, V_m hyperpolarized to a pre-anoxic stage after hyper activity and cells became quiescent. This does not necessarily imply that these neurons recovered from seizure but can occur due to depolarization block in which seizure can be maintained even in the absence of continuous neuronal firing (Bikson *et al*., 2003). While co-antagonisms of $GABA_{A/B}$Rs induced PDS, blocking either $GABA_A$ or $GABA_B$Rs alone did not cause catastrophic depolarization. $GABA_A$ and $GABA_B$Rs have a complementary role in reducing neural excitation (Mann *et al*, 2009). Gabazine significantly reduced conductance and reversed the anoxic depolarization; however, $GABA_B$Rs might prevent the release of excitatory neurotransmitters and excitotoxic cell death even when $GABA_A$Rs are inactive. In the anoxic turtle brain, $GABA_B$Rs predominantly act pre-synaptically and decrease excitatory post-synaptic potentials (EPSPs); especially AMPAergic EPSPs (Pamenter *et al,* 2011). Furthermore, we show that inhibiting $GABA_B$Rs alone does not significantly change the anoxic G_w while blocking $GABA_A$Rs does. This suggests that the major change in conductance brought on by anoxia must occur through $GABA_A$Rs and could explain why application of CGP alone causes no catastrophic depolarization. Activity of $GABA_B$Rs may be crucial to neural survival and limiting excitotoxicity especially if $GABA_A$Rs are inactive; perhaps by decreasing EPSPs and reducing neurotransmitter release (Kuramoto *et al*, 2007; Pamenter *et al.,* 2011; Tao *et al*., 2013).

In conclusion, we report that in anoxic goldfish telencephalic stellate neurons AP_f increases while pyramidal neuron AP_f or potential to generate AP's is decreased. In both neuronal types V_m depolarizes towards the reversal potential for the $GABA_A$ receptor but because E_{GABA} is more depolarizing in stellate neurons it is responsible for the increased activity. Inhibiting both $GABA_A$ and $GABA_B$ receptors induces terminal depolarization of goldfish neurons, highlighting the importance of GABA in anoxia tolerance.

Acknowledgments

The authors would like to thank Dr. Kaori Takehara-Nishiuchi and Dr. Martin Wojtowicz for their valuble insights and critiques during every stage of this study.

Competing Interests

No competing interests declared.

Author contributions

L.T.B. provided all necessary equipment for the study, contributed to experimental design, assisted in data interpretations and revising this manuscript. N. J contributed to study design and performing experiments of this study, data interpretation, drafting and revising the article.

Funding

This study was supported by the Natural Science and Engineering Research Council (NSERC Discovery Grant) to L.T.B.

References

Ben-Ari, Y. (2002). Excitatory action of gaba during development: the nature of the nurture. *Nat. Rev. Neurosci*. **3**, 728-739.

Bickler, P.E. and Buck, L.T. (2007). Hypoxia tolerance in reptiles, amphibians and fishes: life with variable oxygen adaptation. *Annu. Rev. Physiol.* **69**, 145-170.

Bikson, M., Hahn, P.J., Fox, J.E., and Jefferys, J.G. (2003). Depolarization block of neurons during maintenance of electrographic seizures. *J. Neurophysiol.* **90**, 2402-2408.

Blaesse, P., Airaksinen, M.S., Rivera, C., and Kaila, K. (2009). Cation-chloride cotransporters and neuronal function. *Neuron*. **61**, 820-838.

Blanton, M. G., Lo Turco, J. J. and Kriegstein, A. R. (1989). Whole cell recording from neurons in slices of reptilian and mammalian cerebral cortex. *J. Neurosci.Methods*. **30**, 203-210.

Buck, L.T. and Hochachka, P.W. (1993). Anoxic suppression of Na(+)-K(+)-ATPase and constant membrane potential in hepatocytes: support for channel arrest. *Am. J. Physiol*. **265**, 1020-1025.

Carling, D. (2004). The AMP-activated protein kinase cascade--a unifying system for energy control. *Trends. Biochem. Sci.* **29**, 18-24.

Connors, B.W., and Kriegsten, A.R. (1986). Cellular physiology of the turtle visual cortex: distinctive properties of pyramidal and stellate neurons. *J. Neurosci.* **6**, 164-177.

Dukoff, D.J., Hogg, D.W., Hawrysh, P.J. and Buck, L.T. (2014) Scavenging ROS dramatically increases NMDA receptor whole cell currents in painted turtle cortical neurons. *J. Exp. Biol.***217**, 3346-3355.

Edwards, R.A., Lutz. P.L., and Baden, D.G. (1988). Relationship between energy expenditure and ion channel density in the turtle and rat brain. *Am. J. Physiol.* **257**, 1354-1358.

Ellefsen, S., Stenslokken, K.O., Fagernes, C.E., Kristensen, T.A., and Nilsson, G.E. (2009). Expression of genes involved in GABAergic neurotransmission in anoxic crucian carp brain (*Carassius carassius*). *Physiol. Genomics.* **36**, 61-68.

Erecinska, M. and Silver, I.A. (1994). Ions and energy in mammalian brain. *Prog. Neurobiol.***43**, 37-71.

Errington, A.C., Di Giovani, G., and Crunelli, V. (2014). *Extrasynaptic $GABA_A$ receptors*. Springer New York Heidelberg Dordrecht London.

Gassmann, M., and Bettler, B. (2012). Regulation of neuronal $GABA_B$ receptor functions by subunit composition. *Nature. Rev. Neurosci*. **13**, 380-394.

Hansen, A.J. (1985). Effect of anoxia on ion distribution in the brain. *Physiol. Rev*. **65**, 101-148.

Hochachka, P.W. (1986). Defense strategies against hypoxia and hypothermia. *Science*. **231**, 234-241.

Hochachka, P.W., Buck, L.T., Doll, C.J. and Land, S.C. (1996). Unifying theory of hypoxia tolerance: molecular/metabolic defense and rescue mechanisms of surviving oxygen lack. *PNAS*. **93**, 9493-9498.

Hogg, D.W., Pamenter, M.E., Dukoff, D.J. and Buck, L.T. (2015). Decreases in mitochondrial reactive oxygen species initiate $GABA_A$ receptor- mediated electrical suppression in anoxia-tolerant turtle neurons. *J. Physiol.* **593**, 2311-2326.

Howarth, C., Peppiatt-Wildman, C.M. and Attwell, D. (2010). The energy use associated with neural computation in the cerebellum. *J. Cereb. Blood. Flow. Metab.* **30**, 403-414.

Hylland, P. and Nilsson, G.E. (1999). Extracellular levels of amino acid neurotransmitters during anoxia and forced energy deficiency in crucian carp brain. *Brain. Res.* **823**, 49-58.

Johnston, D., and Brown, T.H. (1984). The synaptic nature of the paroxysmal depolarizing shift in hippocampal neurons. *Ann. Neurol*. **16**, 65-71.

Krnjevic, K. (1977). Role of GABA in cerebral cortex. *Can. J. Physiol. Pharmacol*. **75**, 439-451.

Kuramoto. N., Wilkins, M.E., Fairfax, B.P., Revilla-sanchez, R., Terunuma, M., Tamaki, K., Lemata, M., Warren N, Couve A, Calver A, Horvath Z, Freeman K, Carling D, Huang L, Gonzales C, Cooper E, Smart TG, Pangalos M.N. and Moss SJ. (2007) Phospho-dependent functional modulation of GABA(B) receptors by the metabolic sensor AMP-dependent protein kinase. Neuron. 2007 Jan 18; 53(2):233-47.

Larkum, M.E., Watanabe, S., Lasser-Ross, N., Rhodes, P. and Ross, W.N. (2008). Dendritic properties of turtle pyramidal neurons. *J Neurophysiol*. **99,** 683-694.

Lutz, P.L. (1992). Anoxic defense mechanisms in the vertebrate brain. *Annu. Rev. Physiol.* **54**, 601-618.

Lutz, P.L. and Nilsson, G.E. (1997) Contrasting strategies for anoxic brain survival—glycolysis up or down. *J.Exp.Biol.* **200**, 411-419.

Mann, E.O., Kohl, M.M., and Paulsen, O. (2009). Distinct role of $GABA_A$ and $GABA_B$ receptors in balancing and terminating persistent cortical activity. *J. Neurosci*. **29**, 7513-7518.

Megías, M., Emri, Z., Freund, T.F., and Gulyás, A.L. (2001). Total number and distribution of inhibitory and excitatory synapses on hippocampal CA1 pyramidal cells. *Neuroscience*. **102**, 527-540.

Melendez-Ferro, M., Prez-Costas, E. and Roberts, R.C. (2009). A new use for long-term frozen brain tissue: golgi impregnation. *J. Neurosci. Methods*. **176**, 72-77.

Mody, I. (2001). Distinguishing between GABA(A) receptors responsible for tonic and phasic conductances. *Neurochem. Res.* **26**, 907-913.

Muller, T. (2012). What is the thalamus in zebrafish? *Front Neurosci*. doi: 10.3389/fnins.2012.00064

Nakane, R. and Oka, Y. (2010). Excitatory action of GABA in the terminal nerve gonadotropin-releasing hormone neurons. *J. Neurophysiol.* **103**, 1375-1384.

Nilsson, G.E. and Lutz, P. (2004). Anoxia tolerant brains. *J. Cereb. Blood. Flow. Metab.* **24**, 475-486.

Pamenter, M.E., Hogg, D.W., Ormond, J., Shin, D.S., Woodin M.A. and Buck, L.T. (2011). Endogenous $GABA_A$ and $GABA_B$ receptor-mediated electrical suppression is critical to neuronal anoxia tolerance. *PNAS*. **108**, 11274-11279.

Peter. R.E. and Gill. V.E. (1975). A stereotaxic atlas and technique for forebrain nuclei of the goldfish, *Carassius auratus*. *J. Comp. Neurol*. **159**, 69-101.

Sattler, R. and Tymianski, M. (2000). Molecular mechanisms of calcium-dependent excitotoxicity. *J.Mol. Med.* **78**, 3-13.

Shepherd, G.M. (2011). The microcircuit concept applied to cortical evolution: from three-layer to six-layer cortex. *Front. Neuroanat*. doi: 10.3389/fnana.2011.00030.

Shin, D.S. and Buck, L.T. (2003). Effect of anoxia and pharmacological anoxia on whole-cell NMDA receptor currents in cortical neurons from the western painted turtle. *Physiol. Biochem. Zool*. **76**, 41-51.

Stensløkken, K.O.,Ellefsen, S.,Stecyk, J.A.,Dahl, M.B.,Nilsson and G.E.,Vaage, J. (2008). Differential regulation of AMP-activated kinase and AKT kinase in response to oxygen availability in crucian carp (*Carassius carassius*). *Am. J. Physiol. Regul. Integr. Comp. Physiol.* **295**, 1803-1814.

Tao, W., Higgs, M.H., Spain, W.J. and Ransom, C.B. (2013). Postsynaptic GABAB receptors enhance extrasynaptic GABAA receptor function in dentate gyrus granule cells.*J. Neurosci*. **33**, 3738-3743.

Ueno. S., Bracamontes, J., Zorumski, C., Weiss, D.S. and Steinbach, J.H. (1997). Bicuculline and gabazine are allosteric inhibitors of channel opening of the GABAA receptor. *J. Neurosci*. **17**, 625-634.

Warren, N., Couve, A., Calver, A., et al. (2007). Phospho-dependent functional modulation of GABA(B) receptors by the metabolic sensor AMP-dependent protein kinase. *Neuron*. **53**, 233-247.

Watanabe, M., Wake, H., Moorhouse, A.J. and Nabekura, J. (2009). Clustering of neuronal K+-Cl- cotransportes in lipid rafts by tyrosine phosphorylation. *J. Biol. Chem.* **284**, 27980-27988.

Wilkie, M.P., Pamenter, M.E., Alkabie, S., Carapic, D., Shin, D.S. and Buck., L.T. (2008). Evidence of anoxia-induced channel arrest in the brain of the goldfish (*Carassius aratus*). *Comp. Biochem. Physiol. C. Toxicol. Pharmacol.* **148**, 355-362.

Figures

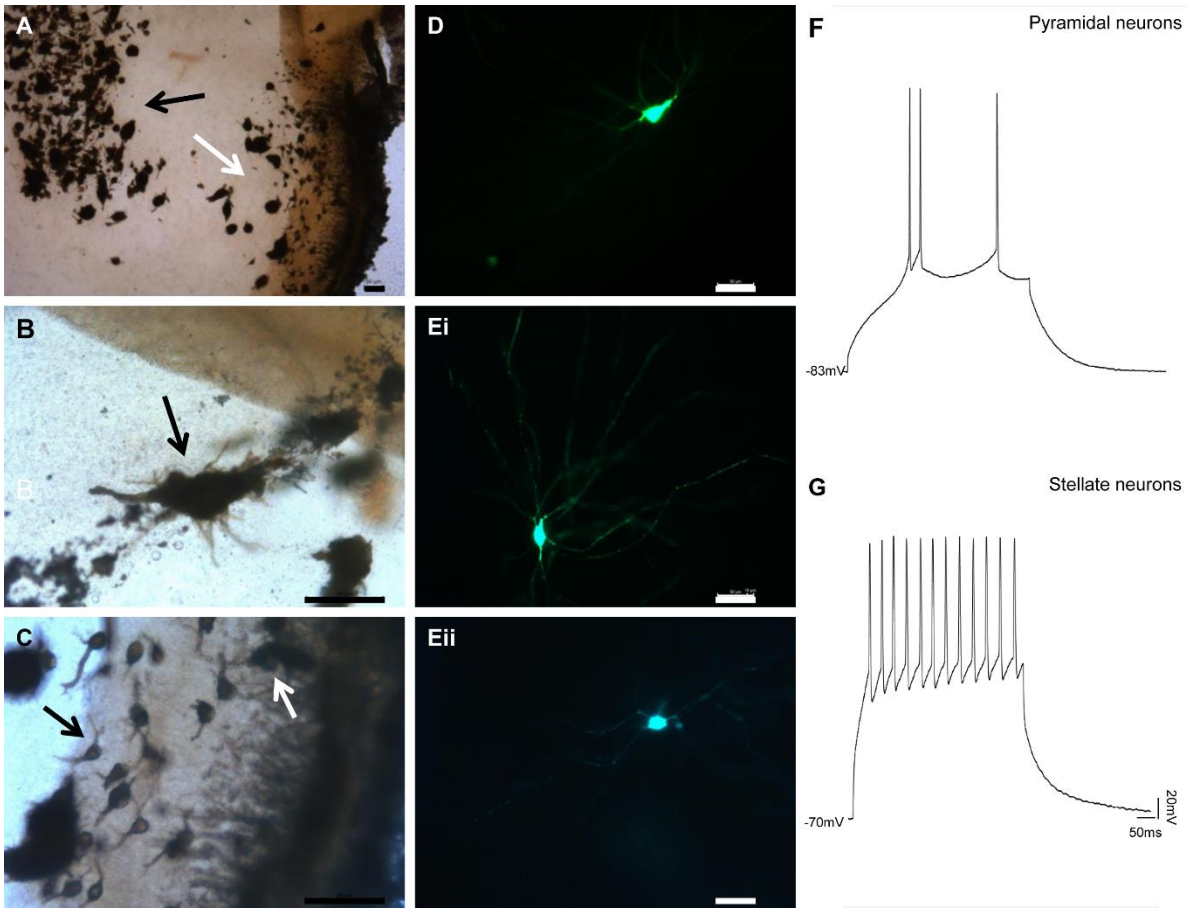

Figure 1. A) An example of Golgi stained goldfish telencephalon slice enlarged 10X. Cells were concentrated at two distinct medial and lateral regions. The two populations were clearly separated by white matter and connective tissue. *Area dorsalis telencephali pars centralis*, pointed to by the black arrow, was the medial region of the slice which contained a large population of pyramidal neurons. The lateral regions, pointed to by white arrow, contained both the small, localized and large stellate cells with medial projections.

B) A pyramidal cell magnified 40X. These cells showed two apical and basal outward projections from their triangular shaped soma.

C) A group of stellate cells with circular shaped somas largely concentrated closer to the edges and appeared to be divided into layers. **D)** A pyramidal neuron filled with Lucifer yellow and imaged

Journal of Experimental Biology • Advance article

immediately after whole-cell recording. These cells expressed the same morphology observed with Golgi staining

E**) (i)** A stellate cell with large dendritic tree and bi-lateral projections. **(ii)** Small stellate neurons that were more concentrated at the lateral region.

F, G) Action potential properties of pyramidal and stellate neurons recorded under current clamp. The pyramidal cells are rapidly adapting neurons while stellate neurons are slowly adapting and can generate action potentials rapidly in response to injected current.

The scale bars represent 50μm.

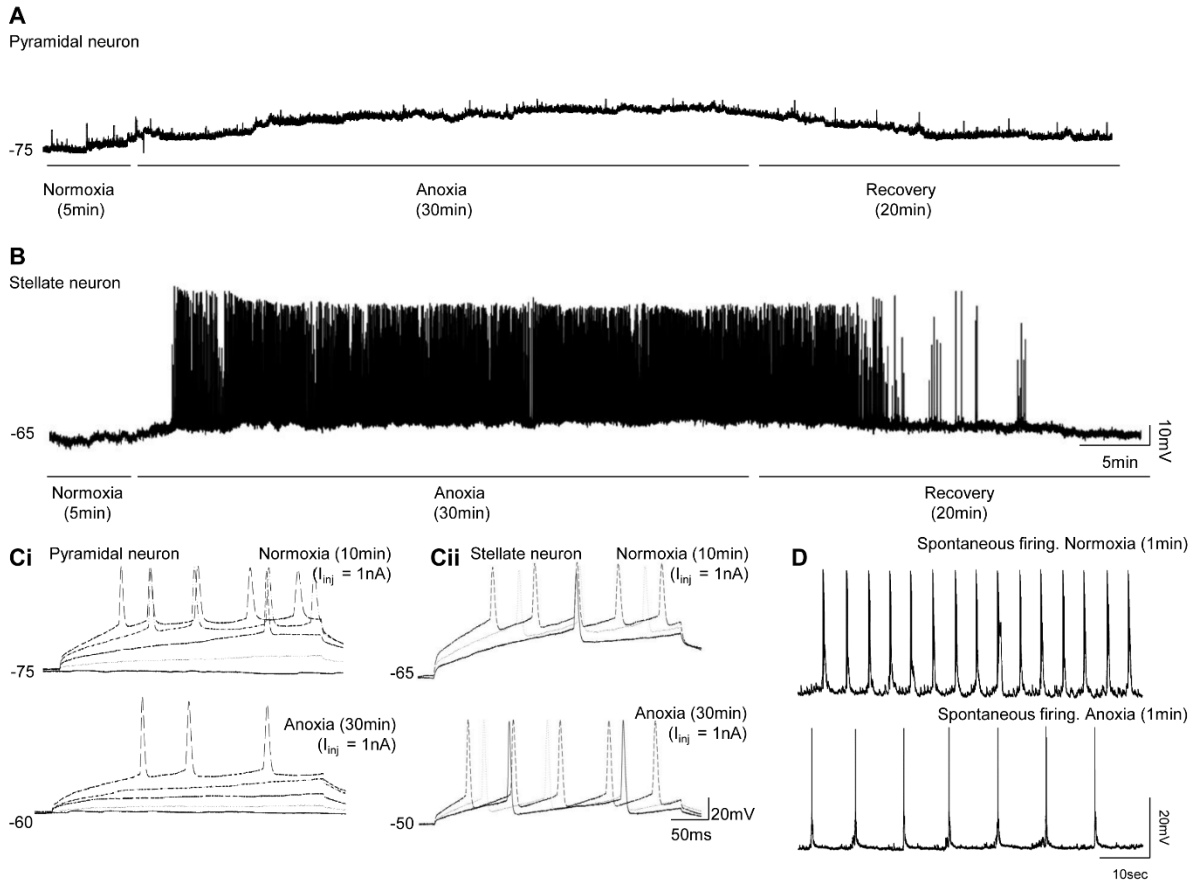

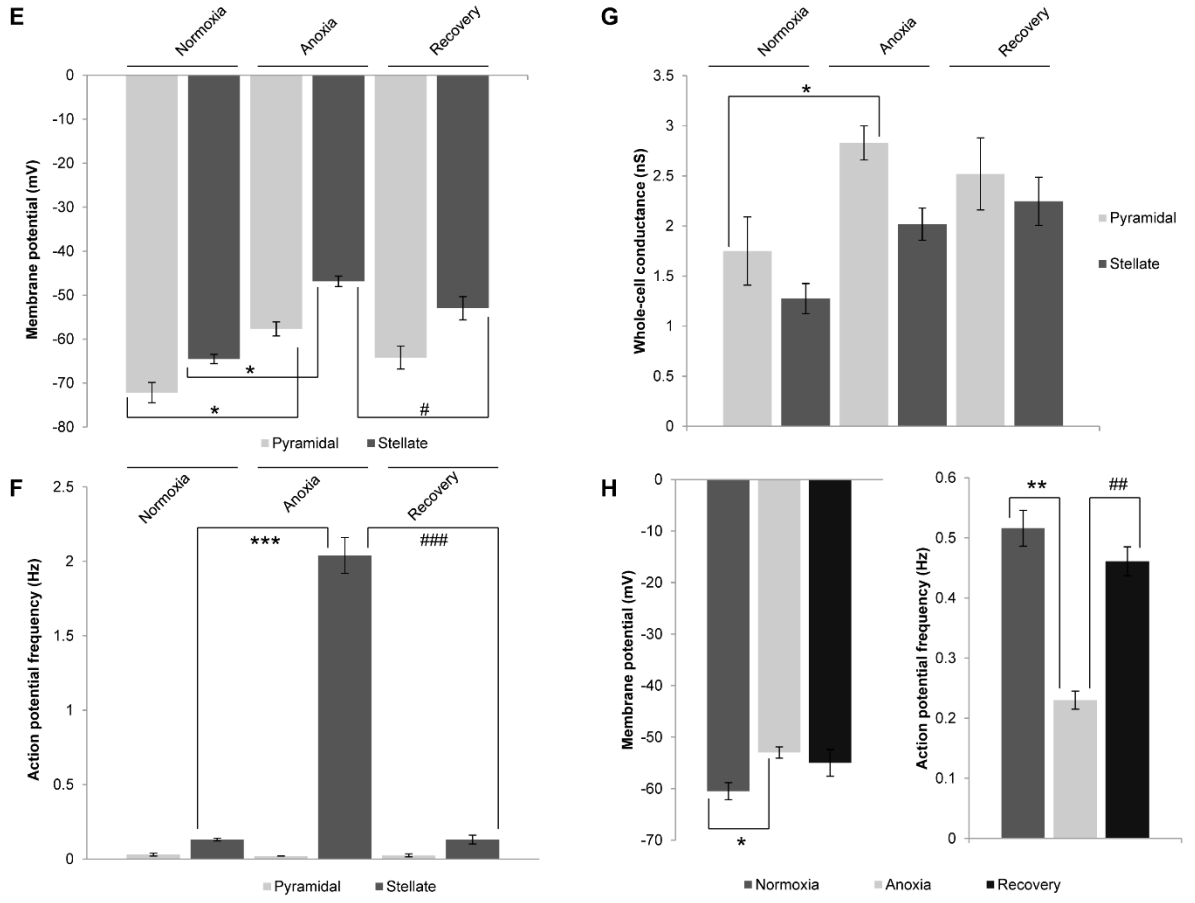

Figure 2. Basic electrophysiological properties of pyramidal and stellate neurons. **A)** Sample trace of free current clamp recording, demonstrating changes in the membrane potnetial (V_m) during normoxia, anoxia and recovery of a pyramidal neuron. **B)** Sample trace of free current clamp, for a stellate neuron showing changes in V_m and action potential frequency (AP_f). **C)** Sample recordings of action potentials by stepwise current injection. **i)** In pyramidal neurons anoxia decreases the probability of action potential generation in response to the same amount of stimulation (1nA). **ii)** Probability of action potential firing did not change with anoxia in stellate neurons; due to membrane potential depolarization firing may have increased. **D)** Occasionally an active pyramidal neurons was found (n=4), a 1 minute example trace of the active neuron during normoxic and then 5 minutes of anoxia is shown. **E)** Summary of changes in: membrane potential, **F)** action potential frequency and **G)** in whole cell conductance (G_w) in both pyramidal and stellate neurons with normoxia, anoxia and recovery. With anoxia (G_w) increased in both cell types. The G_w did not change significantly with recovery in either cell type. **H)** Changes in membrane potential and action potential frequency of active pyramidal neurons as in D. **Treatments:** Normoxia (99% O_2, 1% CO_2 bubbled aCSF), anoxia (99% N_2, 1% CO_2 bubbled aCSF) and recovery (99% O_2, 1% CO_2 bubbled aCSF). Data are mean±S.E.M, n= 7-14 replicates per treatment and n=4 for active pyramidal neurons. Asterisks (*) indicate significant difference from baseline normoxia and the pound sign (#) indicate significant difference from normoxic recovery in pyramidal and stellate neural populations. */# $P<0.05$, **/## $P<0.01$, ***/### $P<0.001$.

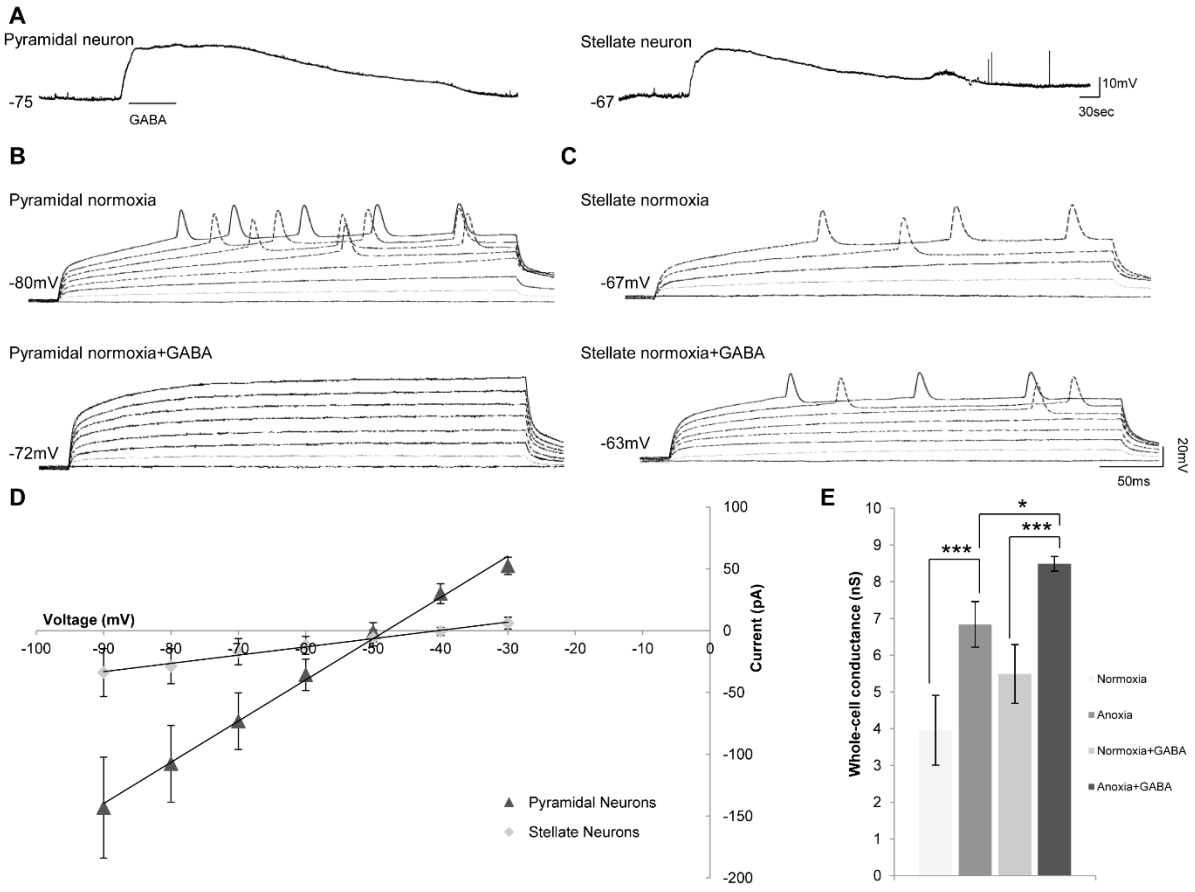

Figure 3. A) Passive recordings from pyramidal and stellate neurons during normoxia and normoxia+GABA. In both neuronal types application of GABA increases the membrane potential (V_m) during normoxia and V_m recovers to the initial baseline minutes after the termination of GABA application. **B)** Sample recordings of action potentials by stepwise current injection from pyramidal neurons before and after GABA application during normoxia. **C)** Stepwise current injection in normoxic stellate neurons pre and post GABA application. **D)** Whole-cell current-voltage relationship from pyramidal and stellate neurons in response to GABA. Application of GABA shifts the membrane potential towards the GABA reversal potential (E_{GABA}) **E)** Changes in whole-cell conductance (G_W) in both pyramidal and stellate neurons with and without exogenous GABA application during normoxia and anoxia. **Treatments:** Normoxia (99% O_2, 1% CO_2 bubbled aCSF), [GABA] = 2 mM. Data are mean±S.E.M, n = 5-8 replicates per treatment. Asterisks (*) indicate significance, (*) P<0.05, (**) P<0.01 and (***) P<0.001.

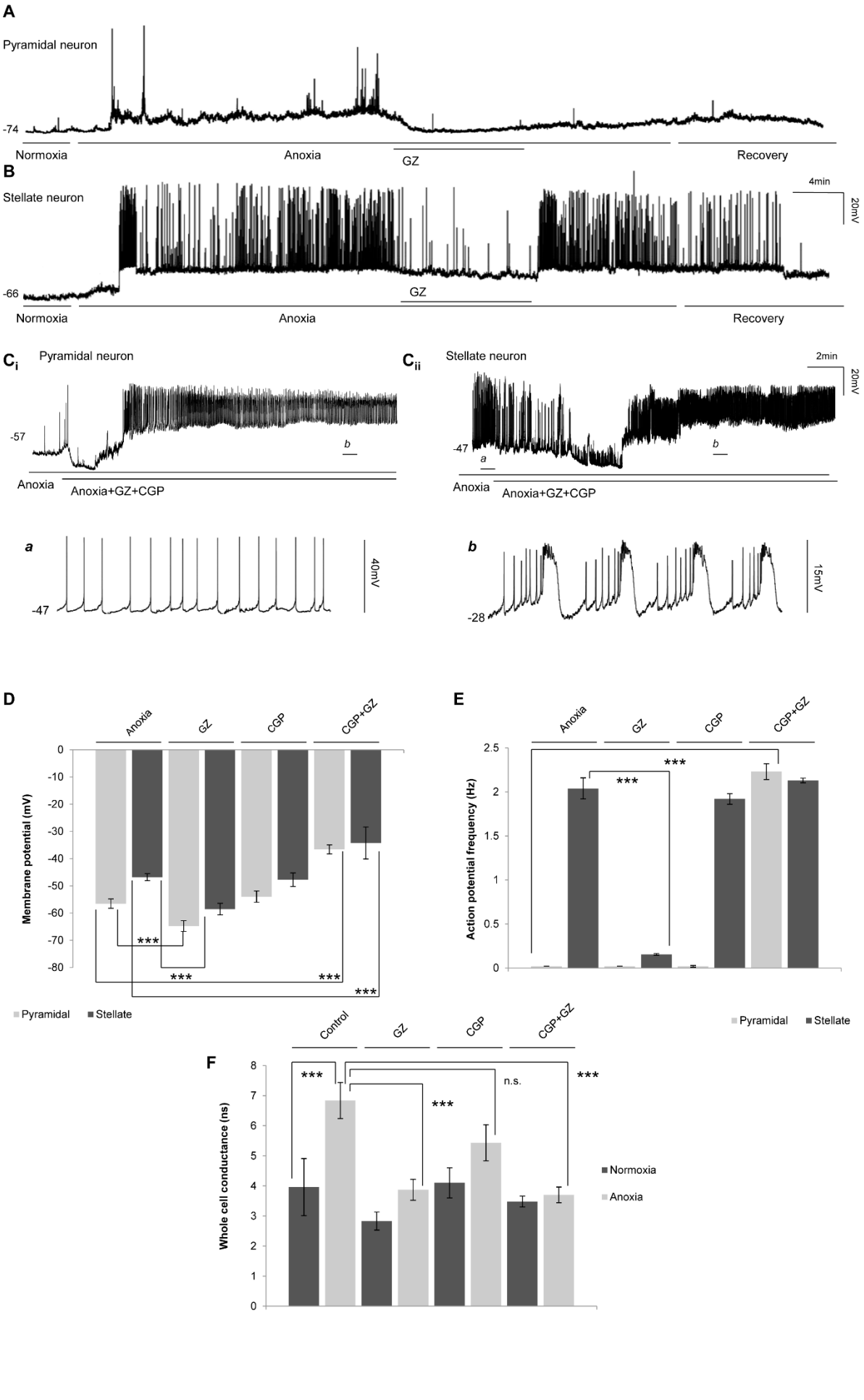

Journal of Experimental Biology • Advance article

Figure 4. Changes in electrophysiological properties in response to GABA receptor inhibition during anoxia. **A)** Application of the GABA-A receptor inhibitor GZ re-polarized pyramidal neuron membrane potential (V_m) back to normoxic levels during anoxic exposure. **B)** Similar to pyramidal neurons GZ re-polarized V_m and reduced action potential frequency (AP_f) in stellate neurons. V_m and AP_f returned to pre-GZ state with normoxic recovery. **$C_{i,ii}$)** Although application of the GABA-B receptor inhibitor CGP-55845 (CGP) alone did not significantly affect V_m or AP_f (data not shown), the combination of GZ+CGP initially hyperpolarized V_m similar to that observed with GZ application. With continuous GZ+CGP application, membrane potential depolarized in both cell types and lead to generation of sudden seizure-like action potentials. ***a,b*** show enlarged traces from represented recordings. **D)** Changes in membrane potential in stellate and pyramidal neurons during anoxia, with application of GZ, CGP-55845 and GZ+CGP. GZ hyperpolarized V_m towards pre-anoxia levels while CGP alone had no significant effects on V_m. GZ+CGP significantly depolarized membrane potential. **E)** Action potential frequency (AP_f) changes with GABA receptor inhibition. GZ had no significant effect on AP_f in pyramidal neurons; however, it significantly reduced AP_f in stellate cells. CGP had no significant effect on AP_f changes in either cell type. GZ+CGP induced seizure-like activities in both neuronal types, significantly increasing the AP_f in pyramidal cells. **F)** Changes in whole-cell conductance (G_w) in both stellate and pyramidal neurons. With anoxia, G_w increased significantly. GZ and GZ+CGP significantly reduced the anoxic G_w while CGP alone, had no significant effect on anoxic conductance. No significant change was observed between pre and post drug application during normoxia. (G_w data were recorded immediately after drug application). **Treatments**: Normoxia (99% O_2, 1% CO_2 bubbled aCSF), anoxia (99% N_2, 1% CO_2 bubbled aCSF). [GZ]=25µM, [CGP] =5µM. n=5-9 for treatment. Asterisks (*) indicate significance, (*) $P<0.05$, (**) $P<0.01$ and (***) $P<0.001$.

List of abbreviations:

aCSF
Artificial cerebrospinal fluid

AMPA
α-amino-3-hydroxy-5-methyl-4-isoxazolepropionic acid

AP_f
Action potential frequency

AP_{th}
Action potential threshold

APV
(2*R*)-amino-5-phosphonovaleric acid

ATP
Adenosine triphosphate

BIC
Bicuculline

CGP
CGP-55848

CNQX
6-cyano-7-nitroquinoxaline-2, 3-Dione

E_{GABA}
GABA reversal potential

GABA
gamma-Aminobutyric acid

$GABA_AR$
GABA-A receptors

$GABA_BR$
GABA-B reptors

G_w
Whole-cell conductance

GZ
Gabazine (SR95531)

NMDA
N-Methyl-D-aspartate

TTX
tetrodotoxin

V_m
Membrane potential

Journal of Experimental Biology • Advance article